Benefiting from polarization – effects on high-NA imaging

Bruce W. Smith, Lena Zavyalova, Andrew Estroff
Rochester Institute of Technology, Microelectronic Engineering Department
82 Lomb Memorial Drive, Rochester, NY

ABSTRACT

The onset of lithographic technology involving extreme numerical aperture (NA) values introduces critical technical issues that are now receiving particular attention. Projection lithography with NA values above 0.90 is necessary for future generation devices. The introduction of immersion lithography enables even larger angles, resulting in NA values of 1.2 and above. The imaging effects from oblique angles, electric field polarization, optical interference, optical reflection, and aberration can be significant. This paper addresses polarization considerations at critical locations in the optical path of a projection system, namely in the illuminator, at the mask, and in the photoresist. Several issues are addressed including TE and azimuthal polarized illumination, wire grid polarization effects for real thin film mask materials, and multilayer resist AR coatings for high NA and polarization.

Keywords: Polarization, optical lithography, high NA, immersion lithography.

1. INTRODUCTION

Optical lithography is being pushed into a regime of extreme-numerical aperture (extreme NA) where polarization effects become important. This paper is a second part in a series addressing polarization effects in optical lithography. The first paper considered the consequences of imaging at numerical apertures at 0.85 with the oblique imaging angles required for low k_1 lithography [1]. A new scaling factor, k_{NA}, was introduced to capture the impact of low k_1 imaging combined with extreme-NA optics and extreme-NA imaging was defined where k_1 and k_{NA} values approach 0.25. Polarization effects combined with resist requirements have been addressed, especially as they relate to 157nm and 193nm lithography. As these technologies are pursued, careful consideration of optical and resist parameters is needed. Conventional targets for resist index, absorption, diffusion, and reflectivity based on normal incidence imaging may not lead to optimum performance without these considerations.

Polarization issues become increasingly important as immersion lithography is considered for next generation optical lithography. The critical implications of immersion lithography are not limited to the lens design, materials, contamination, and fluid control issues that are under exploration as extreme propagation angles are enabled by the technology. As radiation propagates through an optical system, it is influenced by reflection, refraction, and interference (and diffraction). As the polarization state of radiation is considered, it is important to consider the components within the system that can be influenced. Figure 1 shows a schematic of a typical projection imaging system. This paper will address the impact of polarization in three critical locations, namely in the illumination plane, in the mask plane, and in the image plane.

2.0 POLARIZATION AND ILLUMINATION

The benefits of using linearly polarized illumination is realized when the interference of oblique rays is considered. As we move into the regime of extreme NA, methods must be explored that will take full advantage of the potential. Theoretical interference can only occur for radiation propagating in the plane containing the optical axis and perpendicular to the direction of linear propagation (TE polarization). Several approaches to removing field cancellation from TM polarization have been proposed, including image decomposition for polarized dipole illumination [2]. Alternatively, illumination which is consistently TE polarized in a circular pupil could achieve TE polarization for any object orientation. This is possible with an illumination field which is TE polarized over all angles in the pupil, known as azimuthal polarization, which is shown in Figure 2. Such an arrangement provides for homogeneous coupling of the propagating radiation regardless of angle or orientation.

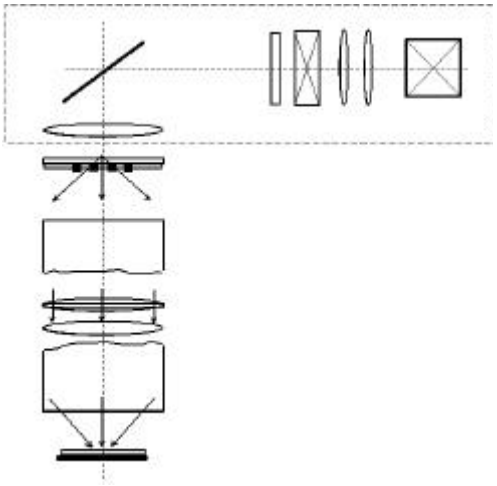

Figure 1. Schematic of polarization critical areas of a projection lithography system.

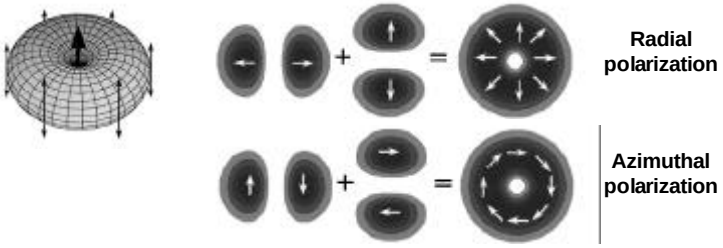

Figure 2. Radial and azimuthal polarization states.

To evaluate the benefits of polarized illumination, a comparative study has been carried out. Figure 3 through 10 show vector image simulation of intensity images in resist using a Prolith/8 model. In all cases, a wavelength of 193nm is used with an immersion NA of 1.2. The resist index used is 1.70 and the immersion fluid index is 1.44 (water). A mask consisting of a pair of five-bar targets is simulated under various conditions of illumination, summarized as follows:

1. Figure 3 shows images from unpolarized dipole illumination. The illumination parameters include a σ_c of 1.0 and a σ_r of 0.25, which is the optimum illumination condition for this pitch, wavelength, and NA condition. The resulting contrast ($[I_{max} - I_{min})/ (I_{max} + I_{min})$] for vertical features is 0.42, which should be adequate for a photoresist to capture, which may need minimum contrast of 0.30 [1]. Horizontal features cannot be resolved.
2. Figure 4 shows images from unpolarized cross-quadrupole illumination [3]. The illumination parameters provide a σ_c of 1.0 and a σ_r of 0.25. The resulting contrast for both vertical and horizontal features is 0.23 which is not likely adequate for imaging.
3. Figure 5 shows images using X-oriented dipoles with Y-oriented polarization. This situation provides for TE polarization across vertical features and TM polarization across horizontal features. The illumination parameters provide a σ_c of 1.0 and a σ_r of 0.25. The resulting contrast for vertical features is high at 0.69 while contrast for horizontal features is zero.
4. Figure 6 shows images using Y-oriented dipoles with X-oriented polarization. This situation provides for TM polarization across vertical features and TE polarization across horizontal features. The illumination parameters provide a σ_c of 1.0 and a σ_r of 0.25. The resulting contrast for vertical features is zero while contrast for horizontal features is high at 0.69.
5. Figure 7 shows images using TE polarized cross-quadrupole illumination. The resulting contrast for both vertical and horizontal features is 0.38, which should be adequate for resolution in resist. Moreover, the contrast is nearly as large as that for the unpolarized dipole case of Figure 3.
6. Figure 8 shows images using unpolarized annular illumination. The illumination conditions of σ_o of 1.0 and a σ_i of 0.80 provide the dipole condition of annular illumination for these 45nm features. Though this approach allows for arbitrary feature orientation, the resulting contrast for both vertical and horizontal features is low at 0.12
7. Figure 9 shows images using TE polarized annular illumination. In this case, the polarization direction provides TE polarization at all angular, or azimuthal, locations around the pupil. Such *azimuthal* polarization combined with an annulus shape allows for the optimum polarization direction of interference for zero and first order diffraction energy for any feature on the mask. The resulting contrast for both vertical and horizontal features is 0.23, which is low for resolution in resist.

8. Figure 10 shows images using TM polarized annular illumination. In this case, the polarization direction provides TE polarization along radial locations in the pupil and TM polarization at any angular location. Such *radial* polarization combined with an annulus shape allows for the non-optimum polarization direction of interference for zero and first order diffraction energy for any feature on the mask. The resulting contrast for both vertical and horizontal features is low at 0.02.

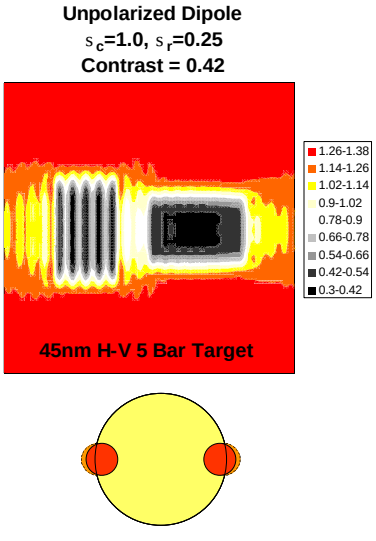

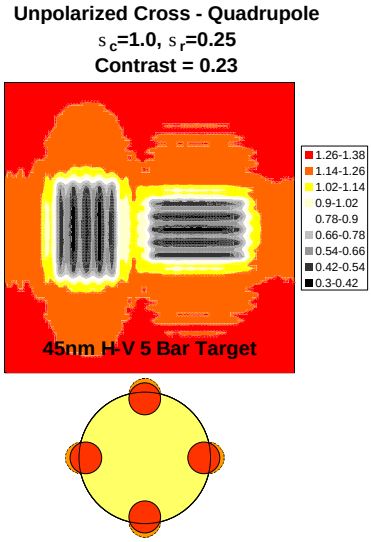

Figures 3 and 4. Resist images of five-bar pattern with unpolarized dipole (L) and cross-quadrupole (R) illumination.

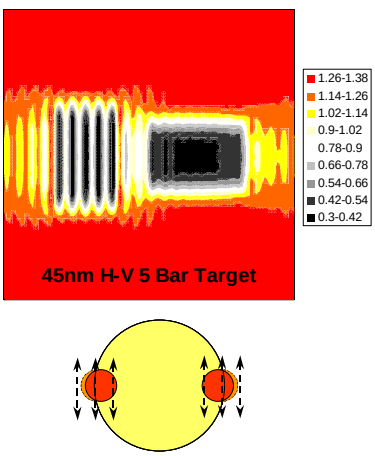

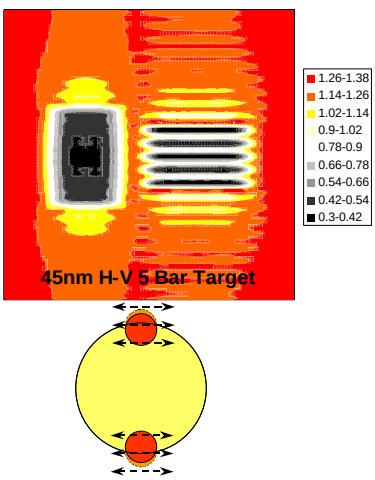

Figures 5 and 6. Resist images of five-bar pattern with Y polarized (L) and X polarized (R) dipole illumination.

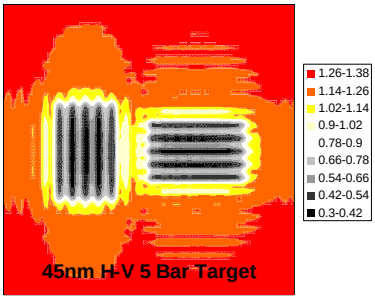

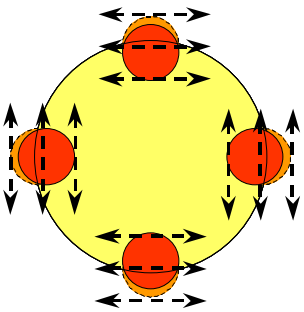

Figure 7. Resist images of five-bar pattern with TE polarized dipole and cross-quadrupole illumination.

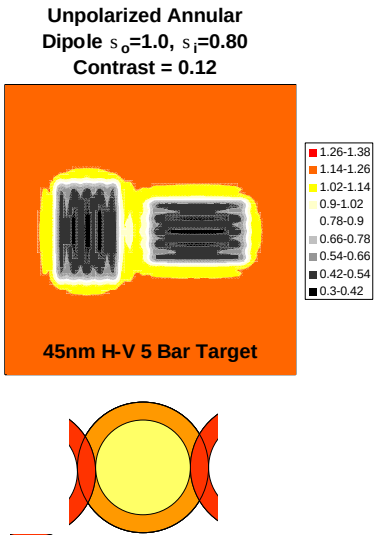

Figures 8 and 9. Resist images of five-bar pattern with unpolarized annular (L) and azimuthal polarized annular (R) illumination.

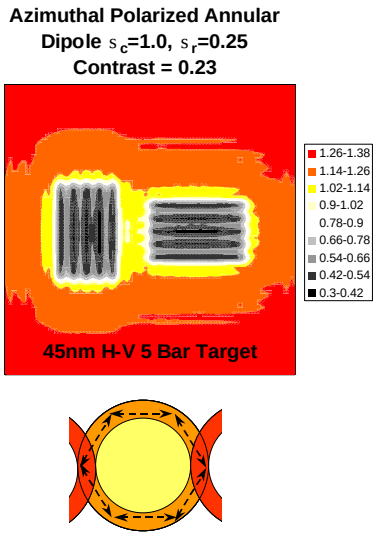

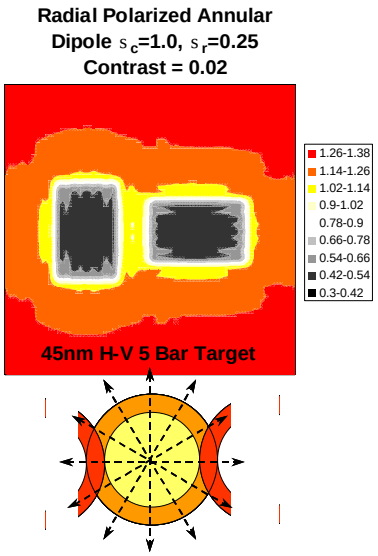

Figure 10. Resist images of five-bar pattern with radial polarized annular illumination.

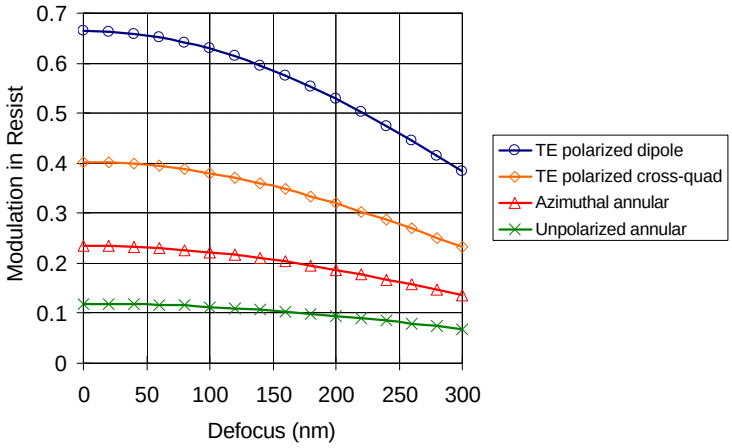

Figure 11. Resist image modulation vs. defocus for several illumination cases of 45nm lines.

Comparison of Figures 7 and 9 show the potential benefit with polarized illumination. Though the azimuthal polarization of Figure 9 can allow for large image contrast for any feature orientation, it is lower than that what is made possible with TE polarized cross-quadrupole illumination. Furthermore, the image contrast for the TE polarized cross-quadrupole is nearly as high as that for the single dipole exposure. Since a dipole exposure would generally require mask decomposition and double exposure, the benefits of the polarized cross-quadrupole are significant.

The situations depicted in Figures 3 through 10 are at best focus. Figure 11 shows the through focus impact for four cases of illumination of these same features. The conditions plotted are for TE polarized dipole, TE polarized cross-quadrupole, azimuthal annular, and unpolarized annular illumination. The TE polarized cross-quadrupole illumination produces contrast values above 0.40 for nearly 300nm of focal depth.

2.1 Polarization experiments at 157nm

Research is underway at 157nm using an Exitech / Tropel small field 0.85 NA projection system where the control of polarization is allowed in the illumination train. This is carried out through the insertion of a polarizing device consisting of pairs of calcium fluoride plates, mounted at Brewster angle, to allow for the control of linear polarization at the mask plane. Through the use of 5 pairs of plates, up to 95% efficiency can be obtained. By reducing the number of pairs, mixed polarization states can also be achieved. This approach allows for the study of the impact of polarization on oblige angle imaging at 157nm. Specifically, half-pitch patterns approaching 60nm are evaluated using RET techniques (alt-PSM and dipole illumination) to understand the effects of polarized illumination. Several methods have been evaluated to achieve polarization in the 157nm system, as described below.

2.1.1 Polarization through birefringence

Polarization can be achieved with crystalline materials that have a different index of refraction in different crystal planes. Such materials are said to be birefringent or doubly refracting. A number of polarizing prisms have been devised which make use of birefringence to separate two beams in a crystalline material. Often they make use of total internal reflection to eliminate one of the planes. The Glan-Taylor, Glan-Thompson, Glan-Laser, beamsplitting Thompson, beam displacing, and Wollaston prisms are most widely used and typically made of nonactive crystals, such as calcite, that transmit well from 350nm to 2300nm. Active crystals such as quartz can also be used in this manner if cut with the optic axis parallel to the surfaces of the plate. It is unlikely that such an approach could be implemented at 157 nm.

2.1.2 Polarization through reflection

The reflection coefficient for light polarized in the plane of incidence is zero at the Brewster angle (sec. 3.1), leaving the reflected light at that angle linearly polarized. This method is utilized in polarizing beamsplitter cubes, which are coated with many layers of quarter-wave dielectric thin films on the interior prism angle to achieve high extinction ratio between the s and p components. Several common types of beamsplitter configurations exist (Wollaston-based broadband, UV laser-line, etc.). However, they are unfeasible for 157 nm applications, as they would require availability of mature high-power durable optical coatings. Perhaps the most promising option here is a Brewster angle plate polarizer that does not require special coatings, and instead, makes use of multiple plane-parallel refracting plates.

It follows from Brewster's law that polarized beam may be formed simply by allowing reflection to take place at the polarizing angle. A plate set at Brewster's angle to the incident beam can thus be used as a polarizer. If a number of plates are stacked parallel, any light reflected from each surface will be TE polarized, and all TM polarized light will be successively transmitted. By making the number of plates within the stack large, high degrees of linear polarization may be achieved. The design that has been utilized is the Brewster-type based of stackable thin plane-parallel CaF2 plates shown in Figure 12. After passing through a sequence of CaF2 plates, the TM (p-polarized) beam will emerge and may be manipulated independently farther down the optical path. To compensate for parallel beam displacement of the output beam that occurs, the plate pairs may be crossed. For propagation from Medium 1 to Medium 2, Brewster's angle is given as $\arctan(n_2/n_1)$. At 157nm, index of refraction for CaF2 is 1.57; hence, the Brewster's angle is 57.3°. Figure 13 shows calculated difference in transmission efficiencies for the two polarization curves. Curves s and p correspond to the response for TE and TM polarization, respectively. Loss is higher for TE compared to TM polarization: after passing two plates, the emerging power is reduced to half (50%) its maximum value. After passing through five pairs of plates, principal transmittance is >99% T for TM (or p) polarization and <3% T for TE (or s) polarization. These values are theoretical and any losses in the system from material absorption or scatter will decrease efficiencies. It is therefore critical that the CaF2 plate components are of the highest VUV quality and are polished to VUV optical lens surface finish specs. Performance specifications for the stacked plate polarizer (of up to 5 pairs) are listed in Table 1. The coupling efficiency of 50% is possible for a single plate pair, versus better than 96% in the limit of five pairs. Theoretical transmission (ratio of total straight through output to total unpolarized input) is 51%. The extinction ratio is 0.03.

Figure 14 shows the initial results of polarized illumination using the CaF_2 Brewster angle polarizer. In this case, 60nm 1:1 duty ratio features are shown from using a binary mask and dipole illumination with 0.77 s_c and 0.1 s_r. TE and TM illumination conditions are shown. Though quantitative analysis remains to be carried out, the improved depth of focus

for the TE polarized condition is evident. Figure 15 shows comparative results for 70nm features imaged with an alternating phase shift mask and TE, TM, and unpolarized illumination with a partial coherence value of 0.3. The focus steps for the TE case are 100nm while the steps for TM and unpolarized illuminations are 50nm, confirming the gain in focal depth achieved with TE polarization.

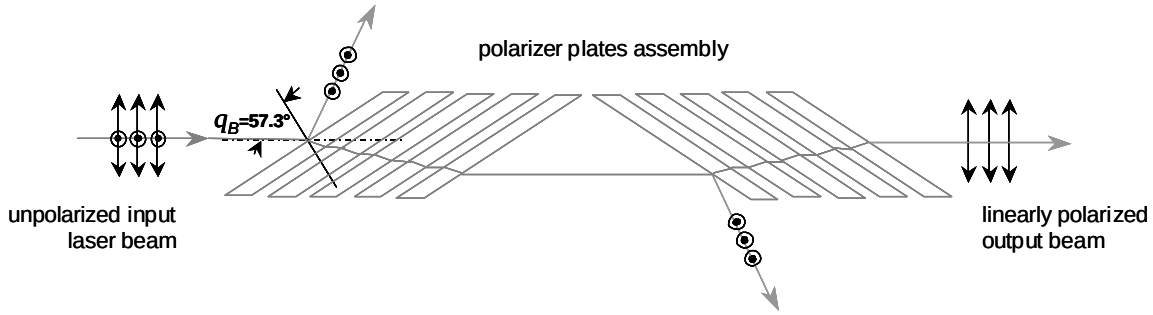

Figure 12. Configuration of Brewster plate polarizer.

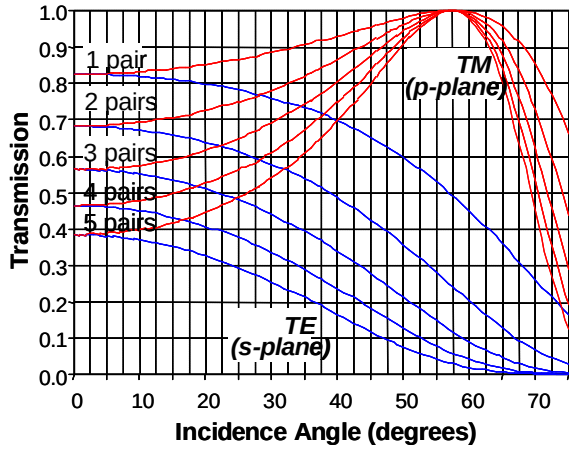

Figure 13. Brewster plate polarizer transmission performance.

	Efficiency 1-T(s)/T(p)	Extinction T(s)T(p)	Transmission [T(p)+T(s)]/2
1 pair	0.500	0.500	0.750
2 pairs	0.750	0.250	0.625
3 pairs	0.875	0.125	0.562
4 pairs	0.938	0.062	0.531
5 pairs	0.969	0.031	0.515

Table 1. Brewster plate polarizer performance data.

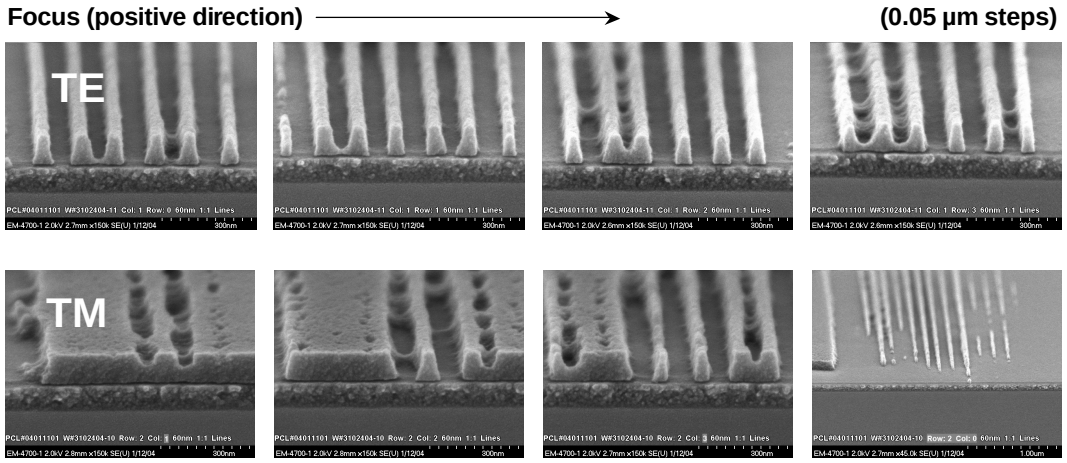

Figure 14. Resist images of 60nm 1:1 features using a binary mask and dipole illumination ($0.77s_c/0.1s_p$).

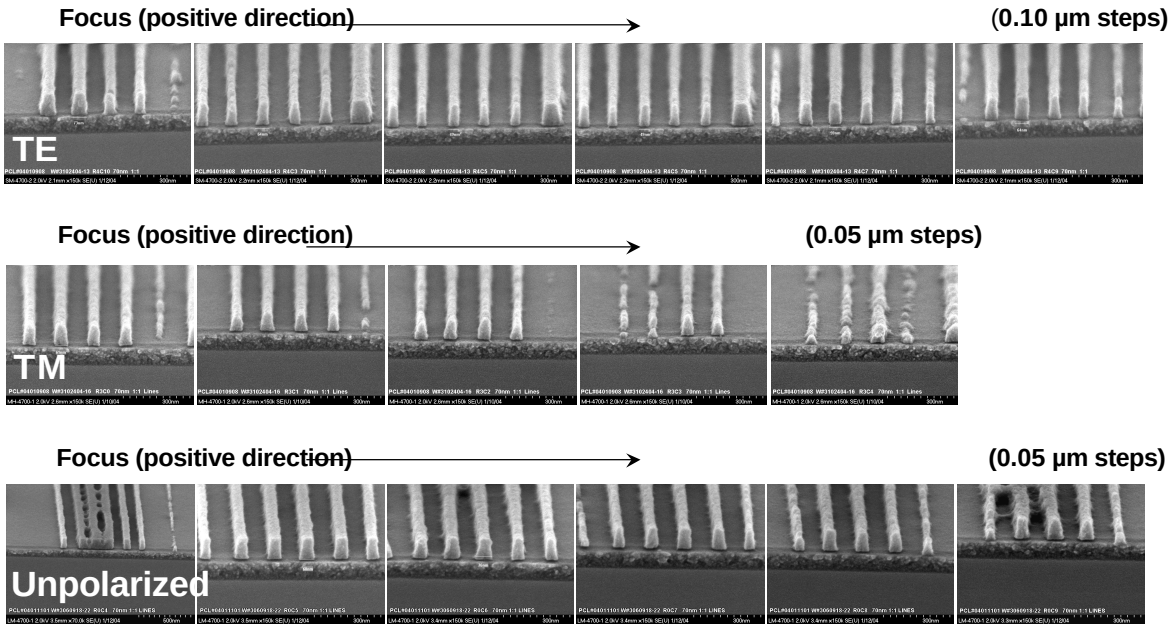

Figure 15. Resist images of 70nm 1:1 features using an alternating phase shift mask and 0.3 s illumination.

3.0 MASK POLARIZATION EFFECTS

We reported on the polarization effects of mask features earlier and expand on these concepts here [1]. Additional analysis is also described in a companion paper [4].

Features on a photomask can begin to influence the polarization as their size approaches the wavelength of illumination. This is a phenomenon of wire grid polarization. Wire grids, generally in the form of an array of thin parallel conductors supported by a transparent substrate, have been used as polarizers for the visible, infrared and other portions of the electromagnetic spectrum. The key factor that determines the performance of a wire grid polarizer is the relationship between the center-to-center spacing, or period, of the parallel grid elements and the wavelength of the incident radiation. If the grid spacing or period is long compared to the wavelength, the grid functions as a diffraction grating, rather than as a polarizer, and diffracts both polarizations (not necessarily with equal efficiency) according to well-known principles. When the grid period is much shorter than the wavelength, the grid functions as a polarizer that reflects electromagnetic radiation polarized parallel to the grid elements, and transmits radiation of the orthogonal polarization.

The transition region, where the grid period is in the range of roughly one-half of the wavelength to twice the wavelength, is characterized by abrupt changes in the transmission and reflection characteristics of the grid. In particular, an abrupt increase in reflectivity, and corresponding decrease in transmission, for light polarized orthogonal to the grid elements will occur at one or more specific wavelengths at any given angle of incidence. These effects were first reported by Wood in 1902 and are often referred to as "Wood's Anomalies" [5]. Subsequently, Rayleigh analyzed Wood's data and had the insight that the anomalies occur at combinations of wavelength and angle where a higher diffraction order emerges. Rayleigh developed the following equation to predict the location of the anomalies (which are also commonly referred to as "Rayleigh Resonances"):

$$\lambda = p\,(n +/- \sin\theta)/m$$

where p is the grating period; n is the refractive index of the medium surrounding the grating; m is an integer corresponding to the order of the diffracted term that is emerging; and λ and θ are the wavelength and incidence angle (both measured in air) where the resonance occurs. For gratings formed on one side of a dielectric substrate, n in the above equation may be equal to either 1, or to the refractive index of the substrate material. The effect of the angular dependence is to shift the transmission region to larger wavelengths as the angle increases. This is important when the polarizer is intended for use as a polarizing beam splitter or polarizing turning mirror.

3.1 Mask thin film structure and polarization

Rigorous coupled-wave analysis (RCWA) is used to study the interaction of electromagnetic waves with mask features. RCWA allows the dependence of polarization effects of various wavelengths of radiation on grating pitch, profile, material, and thickness to be studied. GSOLVER [6] is a visual grating structure editor utilizing full three-dimensional vector code using hybrid RCWA and modal analysis and was used to carry out analysis. The code is capable of analyzing arbitrary grating thickness, number of materials, and material index of refraction. Additionally, it is capable of modeling multiple materials, buried structures, and varied shapes (represented by stacked layers).

Mask features can be approximated by assuming that they are a grating of a thin film material on a dielectric substrate. A binary CrxOyNz-on-glass mask has been modeled using an effective media approximation of data from sputtered thin films [6]. Although CrxOyNz-on-glass masks are typically graded structures, as seen in Figure 16, the four layer stack used in this experiment properly represents this. Tables 2 and 3 contain details of the structure and properties of the films modeled. Figures 17 and 18 show the 193nm transmission and polarization effects of zero and first diffraction orders. The degree of polarization (DoP) is defined as the normalized transmission ratio of polarization states:

$$DoP = \frac{T_{TE} - T_{TM}}{T_{TE} + T_{TM}}$$

where negative values imply TM polarization and positive values imply TE polarization. As the period approaches λ, first diffraction orders are eliminated and the structure becomes a zero-order grating. While polarization of zero order is TM with decreasing pitch, first order is polarized TE which a DoP as large as 20%

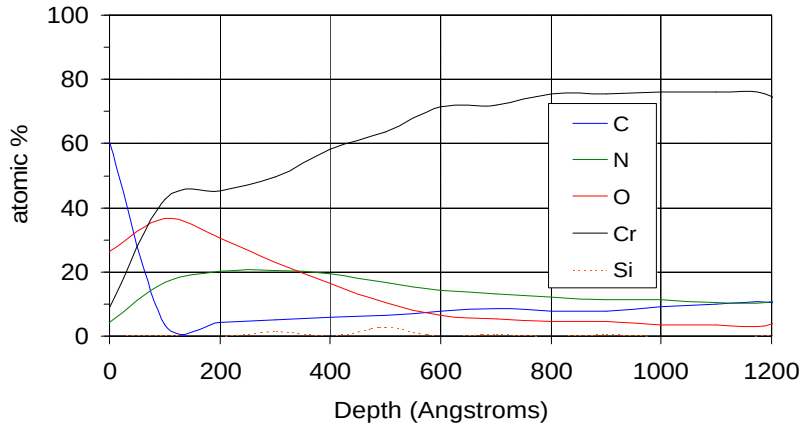

Figure 16. CrxOyNz graded binary mask film composition from XPS analysis.

Attenuated Phase Shifting Mask (APSM) materials were also modeled. APSM materials chosen were Tantalum Nitride in a Silicon Nitride host (TaN-Si3N4), Molybdenum Oxide in a Silicon Dioxide host (MoO3- SiO2), Silicon in a Silicon Nitride host (Si-Si3N4), and Tantalum Oxide in a Silicon Dioxide host (TaO5-SiO2). These materials were also modeled using an effective media approximation of data from sputtered thin films. All were designed for 10% transmission. Figures 19 and 20 show 193nm results, where first and zero diffraction order polarization are shown to be

influenced by the specific structure of the masking film. Unlike the binary CrxOyNz case, first order polarization can be driven toward TM, with a DoP as large as 50%.

The above examples have utilized normal incidence illumination. In reality, the mask is subjected to illumination at angles determined by the partial coherence factor and system magnification. By assuming a 1.2NA projection system and a 4X reduction, an oblique angle of 17.45° in air (and 11.5° in the mask substrate) results. Figures 21 and 22 show the impact that oblique illumination on orders. As illumination angle increases, the first diffraction order closest to the illumination angle begins to resemble the zero order while the farthest order begins to posses second order behavior. Asymmetrical affects impact DoP as well as cut-off period. This will likely influence lithographic effects and warrants further study.

	Cr-O-N Stack Composition			
	Layer 1	Layer 2	Layer 3	Layer 4
Cr	90.00%	18.90%	9.45%	0.00%
CrN	10.00%	2.10%	1.05%	0.00%
CrOx	0.00%	79.00%	89.50%	100.00%

	Data for Cr-O-N Stack (Layer 1 is closest to substrate, Layer 4 is furthest)							
	Layer 1		Layer 2		Layer 3		Layer 4	
	193nm	248nm	193nm	248nm	193nm	248nm	193nm	248nm
n	0.8209	0.8863	1.5649	1.8142	1.6740	1.9734	1.7782	2.1260
k	1.1825	1.8700	0.4121	0.7391	0.3597	0.6584	0.3148	0.5918
Thickness (A)	900	900	133	133	133	133	133	133

Tables 2 and 3. Details of the structure and properties of the CrxOyNz films modeled.

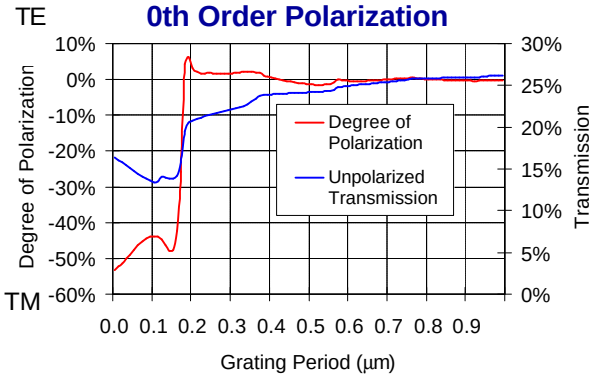

Figure 17. 193nm transmission and polarization effects of the zero diffraction order from CrxOyNz film.

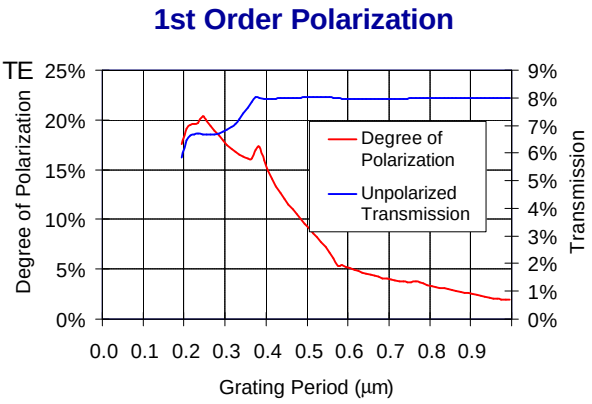

Figure 18. 193nm transmission and polarization effects of first diffraction orders from CrxOyNz film.

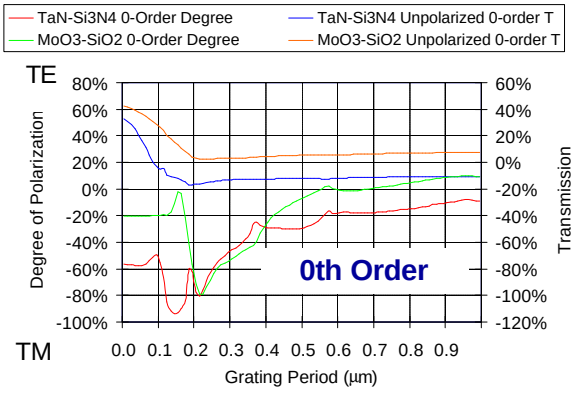

Figure 19. 193nm transmission and polarization effects of the zero diffraction order from APSM films.

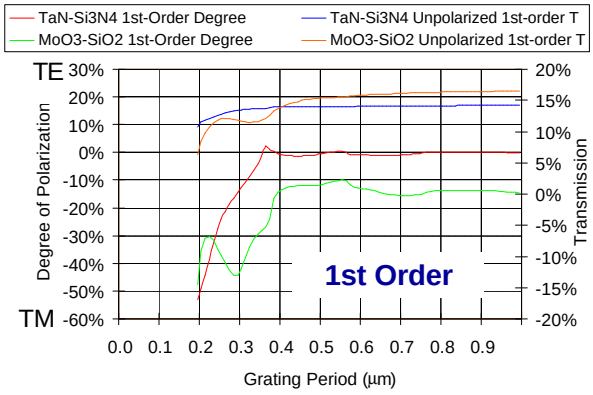

Figure 20. 193nm transmission and polarization effects of first diffraction orders from APSM films.

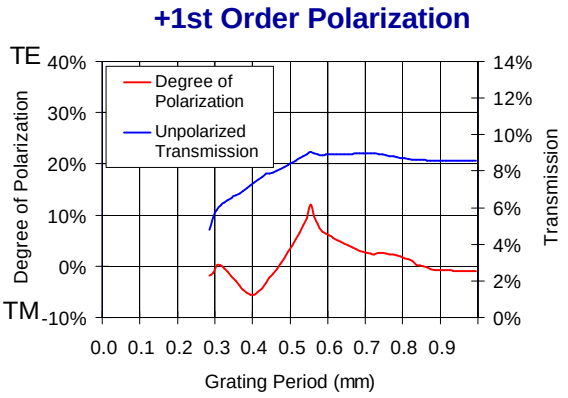

Figure 21. 193nm transmission and polarization effects of +first diffraction order from CrxOyNz film.

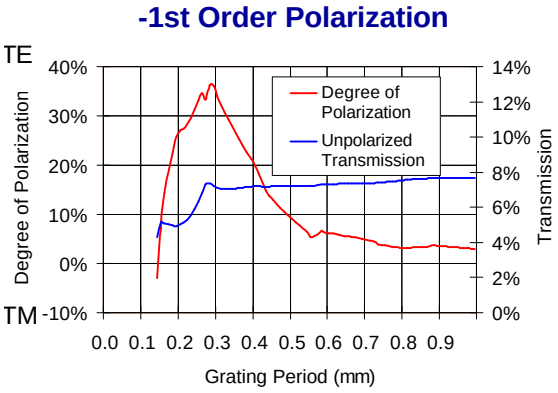

Figure 22. 193nm transmission and polarization effects of -first diffraction order from CrxOyNz film.

4.0 THIN FILMS REFLECTION EFFECTS

To reduce the reflectivity at an interface between a resist layer and a substrate, a bottom anti-reflective coating (BARC) is coated between beneath the resist [7]. Interference minima occur as reflectance from the BARC/substrate interface interferes destructively with the reflection at the resist/BARC interface. This destructive interference thickness repeats at quarter wave thickness. Figure 23 is a series of plots of substrate reflectivity for a 193nm resist as a single layer BARC optical properties (n and k) and thickness are varied over a range comparable to those available to a lithographic process. These plots are for normal incidence, which is not necessarily a good predictor for reflectivity effects at high NA. Figure 24 shows plots for unpolarized 45° incidence in the resist, which would be expected for a numerical aperture of 1.2 and a resist index of 1.70. The location of extent of the nodes are significantly influenced. Figure 25 shows plots for TE polarization and Figure 26 shows TM polarization (where the unpolarized case is the sum of TE and TM).

Optimization of a single layer BARC is possible for oblique illumination and also for specific cases of polarization, as seen in the plots of Figure 27. The issue with a single layer AR film, however, is its inability to achieve low reflectivity across all angles and through both states of linear polarization. This can be achieved using a multilayer BARC design, as shown in Figure 28. By combining two films in a stack and optimizing their optical and thickness properties, reflectivity below 0.6% can be made possible for angles to 45° (1.2NA) for all polarization states, as shown in Figure 29.

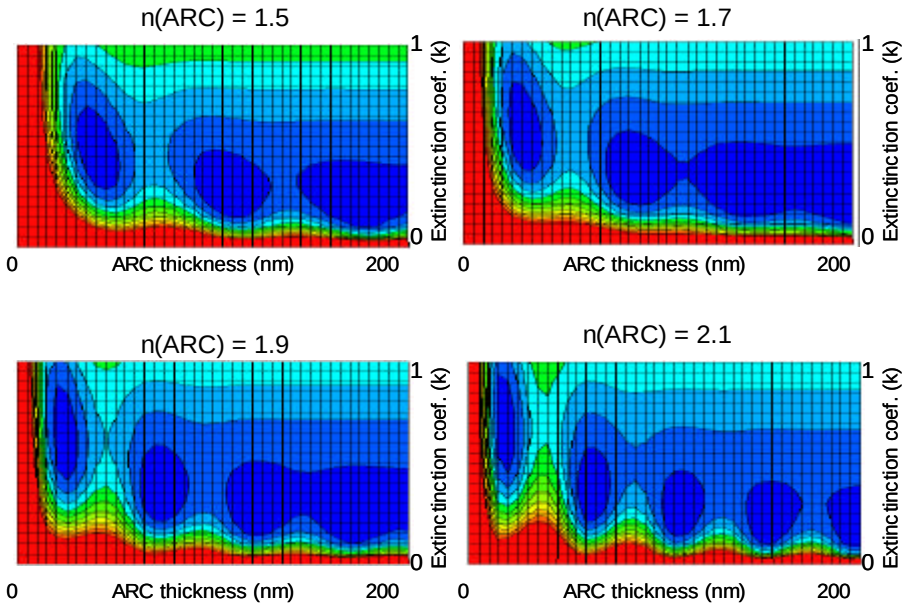

Figure 23. Reflectivity contour plots for 193nm BARC films under resist at

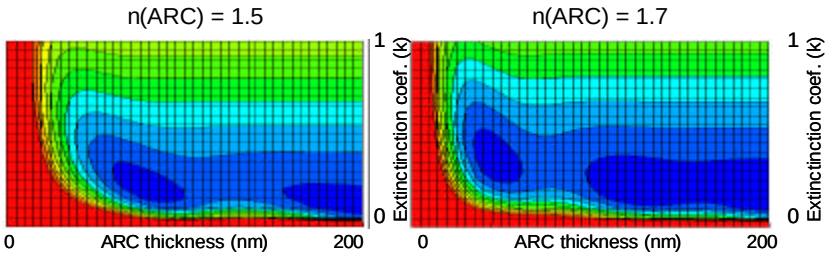

Figure 24. Reflectivity contour plots for 193nm BARC films under resist at 45 ° incidence with unpolarized

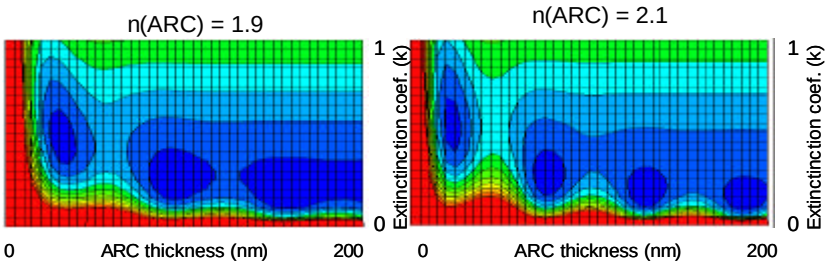

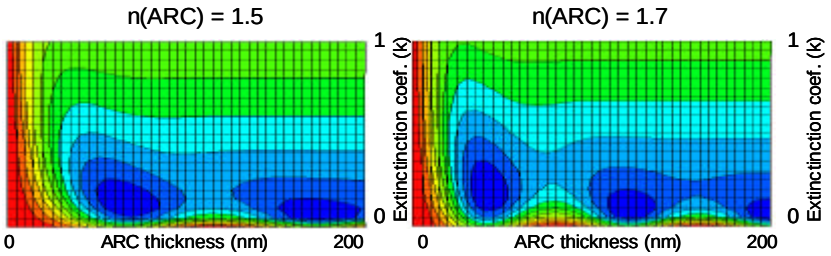

Figure 25. Reflectivity contour plots for 193nm BARC films under resist at 45 ° incidence with TE polarized illumination

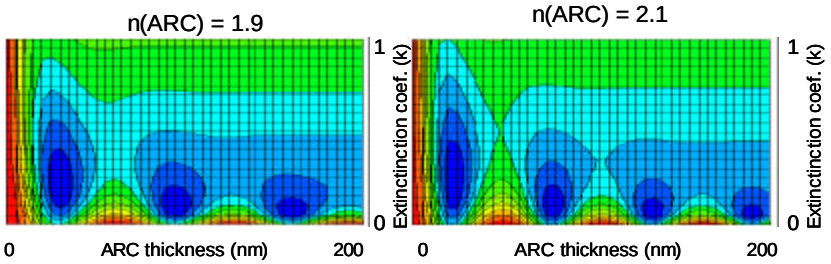

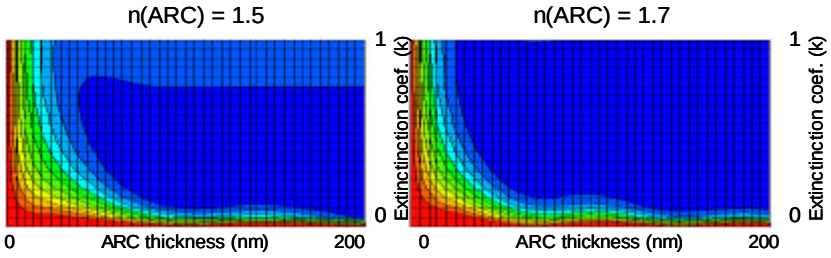

Figure 26. Reflectivity contour plots for 193nm BARC films under resist at 45 ° incidence with TM polarized illumination

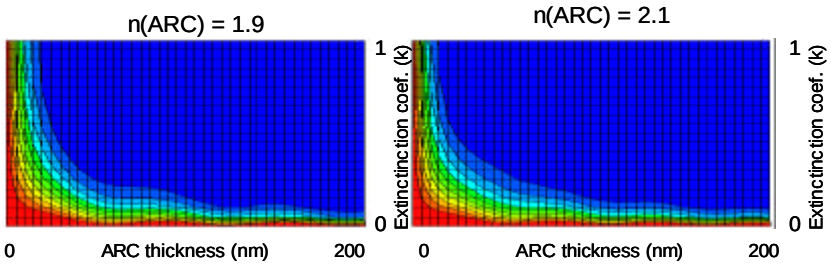

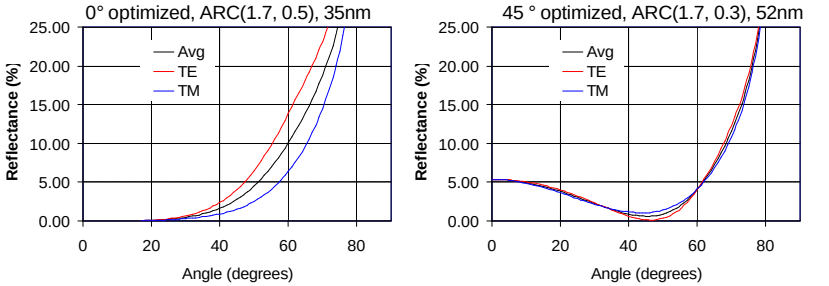

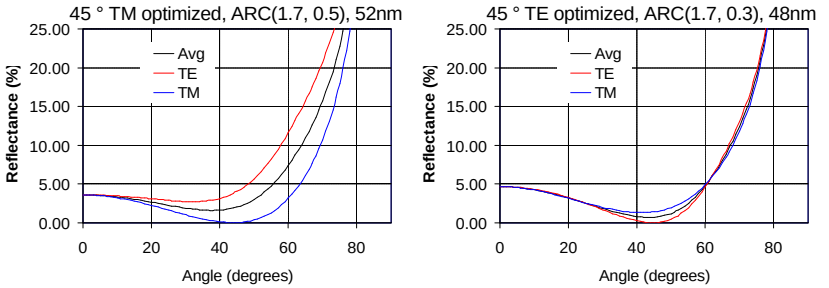

Figure 27. Optimization of reflectivity for single layer BARC films.

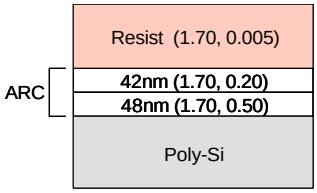

Figure 27. Optical stack configuration for a dual layer BARC.

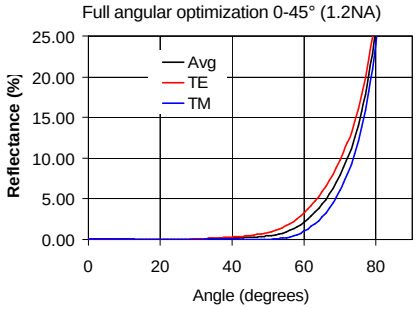

Figure 29. Optimization of reflectivity for a dual layer BARC film.

5.0 CONCLUSIONS

Several critical polarization issues have been discussed as they relate to the optical path of a projection system, namely in the illuminator, at the mask, and in the photoresist. The challenges involved with the design, implementation, and manufacturing with high NA systems of the future will need to address these issues in order to take full advantage of the potential available with new technologies. The topics addressed, including TE and azimuthal polarized illumination, wire grid polarization effects for real thin film mask materials, and multilayer resist AR coatings for high NA and polarization, present no “show-stopper” issues but will require significant development and engineering effort in the future.

6.0 REFERENCES

[1] B. W. Smith, J. Cashmore , M. Gower, “Challenges in High NA, Polarization, and Photoresists”, Proc. SPIE Optical Microlithography XV, Vol. 4691, 2002.
[2] B. W. Smith, A. Bourov, H. Kang, et al, J. of Microlithogr., Microfabr., and Microsyst 3(1) (2004) 44.
[3] B. W. Smith, US Patent 6,388,736.
[4] A. Estroff, Y. Fan, A. Bourov, F. Cropanese, N. Lafferty, L. Zavyalova, B.W. Smith, “Mask induced polarization,” Proc. SPIE Optical Microlithography XVII, Vol. 5377, 2004.
[5] R. W. Wood, ”Uneven Distribution of Light in a Diffraction Grating Spectrum, Philosophical Magazine, September, 1902.
[6] GSOLVER V4.20b, Grating Solver Development Company, 2004.
[7] B. W. Smith, A. Bourov, L. Zavyalova, M. Cangemi, “Design and development of thin film materials for 157 nm and VUV wavelengths: APSM, binary masking, and optical coatings applications, ", Proc. SPIE Emerging Lithographic Technologies III, 1999.